EARTHQUAKE ENGINEERING AND STRUCTURAL DYNAMICS
Earthquake Engng Struct. Dyn. 2000; **29**: 557–575

Seismic response control of frame structures using magnetorheological/electrorheological dampers

Y. L. Xu[1,*], W. L. Qu[2] and J. M. Ko[1]

[1]*Department of Civil and Structural Engineering, The Hong Kong Polytechnic University, Hung Hom, Kowloon, Hong Kong*
[2]*Institute of Civil Engineering and Architecture, Wuhan University of Technology, Wuhan, People's Republic of China*

SUMMARY

Semi-active control of buildings and structures for earthquake hazard mitigation represents a relatively new research area. Two optimal displacement control strategies for semi-active control of seismic response of frame structures using magnetorheological (MR) dampers or electrorheological (ER) dampers are proposed in this study. The efficacy of these displacement control strategies is compared with the optimal force control strategy. The stiffness of brace system supporting the smart damper is also taken into consideration. An extensive parameter study is carried out to find the optimal parameters of MR or ER fluids, by which the maximum reduction of seismic response may be achieved, and to assess the effects of earthquake intensity and brace stiffness on damper performance. The work on example buildings showed that the installation of the smart dampers with proper parameters and proper control strategy could significantly reduce seismic responses of structures, and the performance of the smart damper is better than that of the common brace or the passive devices. The optimal parameters of the damper and the proper control strategy could be identified through a parameter study. Copyright © 2000 John Wiley & Sons, Ltd.

KEY WORDS: frame structure; seismic response; vibration control; control strategies; smart dampers

1. INTRODUCTION

Conventional seismic design of a frame structure relies on the inherent ductility of the structure to dissipate seismic-generated vibration energy while accepting a certain level of structural damage. An alternative approach to dissipate seismic energy and to prevent catastrophic failure of a frame structure is to install passive or active devices within the structure. Passive devices, such as viscoelastic damper, viscous fluid damper, friction damper, metallic damper, tuned mass damper, and tuned liquid damper can partially absorb structural vibration energy and reduce seismic response of the structure [1]. These passive devices are relatively simple and easy to be complemented. However, the effectiveness of passive devices is always limited due to the passive nature of devices and the random nature of earthquake events. Active devices, including active

*Correspondence to: Y.L. Xu, Department of Civil and Structural Engineering, The Hong Kong Polytechnic, Hung Hom, Kawloon, Hong Kong.

Received 8 June 1999
Accepted 23 September 1999

mass damper and active tendon system, can more effectively reduce seismic structural response than passive devices because feedback and/or feedforward control systems are used [2]. However, the complicated control system and the large power requirement during strong earthquake hamper their implementation in practice. Therefore, different types of semi-active devices have been recently developed to equip passive control devices with actively controlled parameters forming a semi-active yet stable and low-power required damping systems [3]. Among them, MR dampers and ER dampers are two typical types of smart (semi-active) dampers under active research.

MR dampers typically consist of a hydraulic cylinder containing micron-sized magnetically polarizable particles suspended within a fluid. In the presence of strong magnetic field, the particles polarize and offer an increased resistance to flow. By varying the magnetic field, the mechanical behaviour of an MR damper can be modulated. Since MR fluids can be changed from a viscous fluid to a yielding solid within milliseconds and the resulting damping force can be considerably large with a low-power requirement, MR dampers are applicable to large civil engineering structures. ER dampers are essentially electric analogs of MR dampers. ER fluid contains micro-sized dielectric particles and its behaviour can be controlled by subjecting the fluid an electric field. For seismic response control, MR dampers were investigated by Dyke *et al.* [4, 5] Carlson *et al.* [6], Spencer *et al.* [7, 8], and others while ER dampers for seismic response control were studied by Ehrgott and Masri [9], Gavin *et al.* [10, 11], Makris *et al.* [12], and others.

With respect to control strategies of structures with MR dampers, Dyke *et al.* [4] proposed a clipped-optimal force control algorithm with acceleration feedback and obtained excellent results when this algorithm was applied to control a seismically excited three storey scaled building model. More recently, Ribakov and Gluck [13] investigated the effectiveness of ER dampers in mitigating seismic response of frame structures. They used an optimal linear passive control strategy to determine the viscous constant of the ER damper and then use active control strategy to determine control forces. Through numerical simulation they found that ER dampers could reduce the peak displacement response of a seven storey frame structure up to 65 per cent without increases in base shear forces and accelerations.

In this paper, the force–displacement relationship of an MR damper or an ER damper based on a parallel-plate model is first extended to include the stiffness of chevron brace supporting the smart damper. The equations of motion of a multi-storey frame structure with smart damper–brace systems are then established. The clipped optimal displacement control strategy, which is parallel to the clipped optimal force control strategy, and the optimal displacement control strategy with the controller–structure interaction considered are proposed for seismically excited frame structures with MR or ER dampers and compared with the clipped optimal force control strategy. An extensive parameter study is performed in terms of the maximum yield shear stress and the Newtonian viscosity of MR or ER fluids, the brace stiffness, and the earthquake intensity. Finally, the smart dampers and the optimal displacement control strategy with the controller–structure interaction considered are applied to a five-storey reinforced concrete frame structure.

2. FORMULATION

2.1. Damper–brace model

In the case of a steady, fully developed flow, the shear resistance of MR fluids or ER fluids may be modelled as having a friction component augmented by a Newtonian viscosity component, that

is, the so-called Bingham model [10, 12, 8].

$$\tau = \eta\dot{\gamma} + \tau_y \operatorname{sgn}(\dot{\gamma}) \tag{1}$$

where τ is the shear stress in fluid, η is the Newtonian viscosity, independent of the applied electric/magnetic field, $\dot{\gamma}$ is the shear strain rate and τ_y is the yielding shear stress controlled by the applied field.

For the fluid that can be described by the Bingham model, Phillips derived the following fifth-degree polynomial in 1969 to depict the Poiseuille flow of Bingham material in a rectangular duct [10]:

$$P^3 - (1 + 3T)P^2 + 4T^3 + P^2V + \frac{P^2TV^2}{3A^2} = 0 \tag{2}$$

in which

$$P = \frac{bh^3p'}{12Q\eta}, \quad T = \frac{bh^2\tau_y}{12Q\eta}, \quad V = \frac{bhU}{2Q}, \quad A = P - 2T \tag{3}$$

where p' is the pressure gradient, Q is the volumetric flow rate, b is the width of the rectangular plate, h is the gap between two parallel plates and U is the relative velocity of the two plates.

Gavin *et al.* [10] found that Equation (2), which is based on the simple parallel-plate model, is accurate enough for describing the force–velocity behaviour of cylinder ER dampers in an axisymmetric flow field. They also found out the approximate solutions of Equation (2) for either flow-type smart dampers or mixed-type smart dampers. Upon proper manipulation, the relationship between the force P_{d} and velocity $\dot{e}$ of the smart damper can be expressed as follows:

$$P_{\mathrm{d}}(\mathrm{t}) = C_{\mathrm{d}}\dot{e} + F_{\mathrm{d}} \operatorname{sgn}(\dot{e}) \tag{4}$$

in which

$$C_{\mathrm{d}} = C_1 \frac{12\eta L A_{\mathrm{p}}}{bh^3} A_{\mathrm{p}}, \qquad F_{\mathrm{d}} = C_2 \frac{L\tau_y}{h} A_{\mathrm{p}} + P_{\mathrm{y}} \tag{5}$$

For the flow-type damper,

$$C_1 = 1.0, \quad C_2 = 2.07 + \frac{1.0}{1.0 + 0.4T}, \quad T = \frac{bh^2\tau_{\mathrm{y}}}{12A_{\mathrm{p}}\eta\dot{e}} \tag{6}$$

For the mixed-type damper,

$$C_1 = 1.0 - \frac{bh}{2A_{\mathrm{p}}}, \quad C_2 = 2.07 + \frac{1.0}{1.0 + 0.4T} - \frac{1.5V^2}{1.0 + 0.4T^2}, \quad V = \frac{bh}{2A_{\mathrm{p}}} \tag{7}$$

where L is the effective axial pole length, A_{p} is the cross-sectional area of the piston and P_{y} is the mechanical friction force in the damper. Clearly, F_{d} is the function of the yielding shear stress and it can be controlled through the applied field but C_{d} is independent of the applied field.

For frame structures, MR or ER dampers can be placed between the chevron brace and the rigid floor diaphragm as shown in Figure 1(a). In consideration of the stiffness of chevron brace, the mathematical model for smart damper–chevron brace system can be seen as a damper and a spring being connected in series (see Figure 1(b)). When considering the smart damper and the

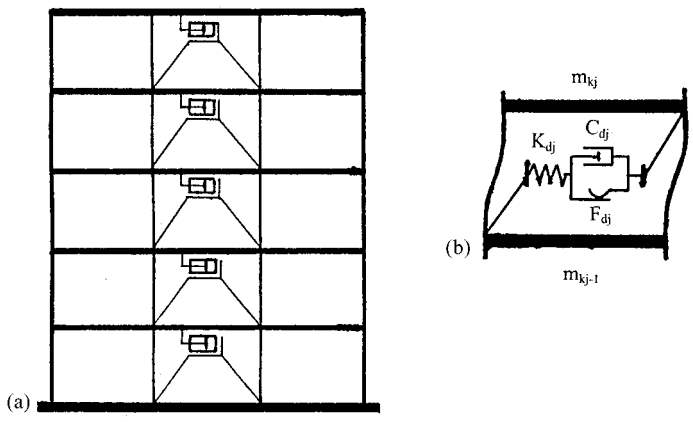

Figure 1. Schematic diagram of smart damper–brace–structure system. (a) frame structure with smart dampers; and (b) mechanical model of smart damper–brace system.

chevron brace to be connected in series, the spring force in the brace is equal to the force on the piston of the damper. Equation (4) should be thus correspondingly changed to

$$C_{\mathrm{d}}\dot{e} + F_{\mathrm{d}}\,\mathrm{sgn}(\dot{e}) = K_{\mathrm{d}}(u - e) \tag{8}$$

where u is the relative displacement between the two floors with the damper installed and K_{d} is the horizontal stiffness of the chevron brace. It is seen that Equation (8) relates the damper force and velocity to the structural displacements.

2.2. *Structure–damper–brace system model*

In terms of Equation (8), equations of motion of an N-storey frame structure with m dampers subject to earthquake excitation can be expressed as

$$[M]\{\ddot{x}\} + [C]\{\dot{x}\} + ([K] + [H][K_{\mathrm{d}}][H]^{\mathrm{T}})\{x\} + [H][K_{\mathrm{d}}]\{e\} = -[M]\{1\}\ddot{x}_{\mathrm{g}}(t) \tag{9}$$

$$\frac{C_{\mathrm{d}_j}}{K_{\mathrm{d}_j}}\dot{e}_j + e_j + \frac{F_{\mathrm{d}_j}}{K_{\mathrm{d}_j}}\,\mathrm{sgn}(\dot{e}_j) = \{H\}_j^{\mathrm{T}}\{x\} = x_{kj} - x_{kj-1} \quad (j = 1, 2, \ldots, m) \tag{10}$$

where $[M]$, $[C]$, and $[K]$ are the $N \times N$ mass, damping, and stiffness matrices of the frame structure; $[K_{\mathrm{d}}]$ is the $m \times m$ diagonal stiffness matrix of which the element is the stiffness coefficient of the chevron brace; m is the number of storeys with smart dampers; $[H]$ is the $N \times m$ matrix converting the brace stiffness matrix into the global co-ordinate system; the superscript T means the transposition of a matrix; $\{x\}$, $\{\dot{x}\}$, and $\{\ddot{x}\}$ are the $N \times 1$ displacement, velocity, and acceleration vectors, respectively, of the frame structure; $\{e\}$ is the $m \times 1$ displacement vector of the dampers: $\{1\}$ is an index vector with all its elements equal to 1; $\ddot{x}_{\mathrm{g}}(t)$ is the ground acceleration; $\{H\}_j$ is the jth column vector of the matrix $\{H\}$; and x_{kj} and x_{kj-1} are the displacements of the top and bottom floors of the kj storey where the jth damper is installed.

Equation (9) can be replaced by an equivalent first-order differential equation of the form

$$\{\dot{Z}\} = [A]\{Z\} + [B]\{e\} + \{D\}\ddot{x}_{\mathrm{g}} \tag{11}$$

in which

$$[A] = \begin{bmatrix} [0] & [I] \\ -[M]^{-1}([K] + [H][K_{\mathrm{d}}][H]^{\mathrm{T}}) & -[M]^{-1}[C] \end{bmatrix} \tag{12}$$

$$[B] = \begin{bmatrix} [0] \\ [M]^{-1}[H][K_{\mathrm{d}}] \end{bmatrix}, \quad \{D\} = \begin{bmatrix} \{0\} \\ -\{1\} \end{bmatrix}, \quad \{Z\} = \begin{bmatrix} \{x\} \\ \{\dot{x}\} \end{bmatrix} \tag{13}$$

Equations (10) and (11) are the basic equations for the semi-active control of seismic response of frame structures with MR or ER dampers using displacement control strategy. Clearly, the motion of the structure is coupled with the motion of the dampers.

To apply force control algorithm, Equations (10) and (11) can be re-written as

$$C_{\mathrm{d}_j}\dot{e}_j + F_{\mathrm{d}_j}\mathrm{sgn}(\dot{e}_j) = K_{\mathrm{d}_j}(x_{kj} - x_{kj-1} - e_j) = U_{Rj} \tag{14}$$

$$\{\dot{Z}\} = [\bar{A}]\{Z\} + [\bar{B}]\{U_R\} + \{D\}\ddot{x}_{\mathrm{g}} \tag{15}$$

in which

$$[\bar{A}] = \begin{bmatrix} [0] & [I] \\ -[M]^{-1}[K] & -[M]^{-1}[C] \end{bmatrix}, \quad [\bar{B}] = \begin{bmatrix} [0] \\ [M]^{-1}[H] \end{bmatrix} \tag{16}$$

3. CONTROL STRATEGIES

3.1. Optimal force control

The linear quadratic regular (LQR) control theory has been extensively used for active control [14, 15] and for semi-active control (e.g. [16]) of structures. In this algorithm, the optimal control force $\{U_T\}$ for $\{U_R\}$ in Equation (15) is selected by minimizing the following performance index:

$$J = \int_0^{t_{\mathrm{f}}} (\{Z\}^{\mathrm{T}}[\bar{Q}]\{Z\} + \{U_R\}^{\mathrm{T}}[\bar{R}]\{U_R\})\,\mathrm{d}t \tag{17}$$

where $[\bar{Q}]$ is the weighting matrix for the structure response; it is an $N \times N$ positive-semi-definite matrix; $[\bar{R}]$ is the weighting matrix for the control force; it is an $m \times m$ positive-definite matrix; and t_{f} is a duration defined to be longer than that of the earthquake which is assumed to be a white noise random process. For a closed-loop control configuration, minimizing Equation (17) subject to the constraint of Equation (15) results in the following optimal control force vector $\{U_T\}$:

$$\{U_T\} = -[\bar{R}]^{-1}[\bar{B}]^{\mathrm{T}}[\bar{P}]\{Z\} \tag{18}$$

where matrix $[\bar{P}]$ is the solution of the classical Riccati equation.

$$[\bar{P}][\bar{B}]^{\mathrm{T}}[\bar{R}]^{-1}[\bar{B}][\bar{P}] - [\bar{A}]^{\mathrm{T}}[\bar{P}] - [\bar{P}][\bar{A}] - [\bar{Q}] = 0 \tag{19}$$

Because the damper force generated in the smart dampers is dependent on the response of the frame structure, the desirable optimal control force U_{Tj} cannot always be produced by the jth damper. Only the damper force, $F_{\mathrm{d}j}$, due to the yielding shear stress in fluids can be controlled through the change in the applied electric or magnetic field. A reasonable approach is thus to

control F_{dj} such that the jth damper force vector U_{Rj} traces the optimal control force U_{Tj} defined by Equation (18) as close as possible. To compare with the subsequent optimal displacement control strategies proposed in this study, the clipped-optimal force control approach (named the control strategy No. 1 in this study) suggested by Dyke *et al.* [4] is adopted as follows. When the jth damper is providing the desired optimal force U_{Tj}, the voltage applied to the damper should remain at the present level. If the magnitude of the force produced by the jth damper U_{Rj} is smaller than the magnitude of the desired optimal force U_{Tj} and the two forces have the same sign, the voltage applied to the damper should be increased to the maximum level. Otherwise, the commanded voltage should be set to zero.

3.2. Optimal displacement control

In parallel to Equation (15), Equation (11) indicates that if we could directly control the displacement vector $\{e\}$ of the smart dampers we could apply the well-developed linear control theories to find the optimal control displacement vector $\{e_T\}$ to minimize the seismic response of the frame structure. Thus, in terms of the linear quadratic regular (LQR) control theory the optimal linear control that minimize

$$J = \int_0^{t_f} (\{Z\}^T[Q]\{Z\} + \{e\}^T[R]\{e\}\,dt \tag{20}$$

is to control the displacement vector $\{e\}$ as

$$\{e_T\} = -[R]^{-1}[B]^T[P]\{Z\} \tag{21}$$

where $[Q]$ is the weighting matrix for the structure response in the optimal displacement control; it is an $N \times N$ positive-semi-definite matrix; $[R]$ is the weighting matrix for the damper displacement in the optimal displacement control; it is an $m \times m$ positive-definite matrix; and $[P]$ is the positive-definite solution of the following Riccati equation:

$$[P][B]^T[R]^{-1}[B][P] - [A]^T[P] - [P][A] - [Q] = 0 \tag{22}$$

As mentioned in the optimal force control, in the present application of smart dampers to frame structures the optimal displacement vector $\{e\}$ cannot be directly controlled. The controllable parameter of the damper is the damper force, F_d, due to the yielding shear stress in fluids. The approach is thus to control F_d such that the measured displacement vector $\{e\}$ traces the optimal displacement vector $\{e_T\}$ defined by Equation (21) as close as possible. According to this principle, the two optimal displacement control strategies are presented in this study. The first one is the clipped optimal displacement control approach which is in parallel to the clipped optimal force control approach (named the control strategy No. 2 in this study), and the second one is the optimal displacement control approach with the controller–structure interaction considered (name the control strategy No. 3 in this study).

The strategy in the clipped optimal displacement control approach can be described as follows. When the jth damper displacement e_j is approaching the desired optimal damper displacement vector e_{Tj}, the friction force F_{dj} in the damper should be set to its minimum value so as to let the jth damper reach its optimal displacement as fast as possible. When the jth damper moves in the opposite direction to the optimal damper displacement, the friction force F_{dj} in the damper should be set to its maximum value so as to prevent the damper motion away from the optimal

target at most. This strategy can be concisely stated as

$$F_{dj} = \begin{cases} F_{min} & \text{when } \dot{e}_j(e_{Tj} - e_j) \succ 0 \\ F_{max} & \text{when } \dot{e}_j(e_{Tj} - e_j) \prec 0 \end{cases} \quad (j = 1, 2, \ldots, m) \tag{23}$$

where F_{max} and F_{min} can be achieved by adjusting the electric or magnetic field to let the yielding shear stress in fluids reach τ_{ymax} and τ_{ymin}, respectively.

In the clipped optimal displacement control approach, when F_{max} is applied to the jth damper but the jth damper force magnitude $K_{dj}(x_{kj} - x_{kj-1} - e_j)$ is less than F_{max} the jth damper will stop moving and no vibration energy can be dissipated. In such a situation, the damper–brace system becomes a common brace and the smart damper loses its effectiveness. To overcome this problem, the clipped optimal displacement control strategy can be modified as follows. When the jth damper displacement e_j is approaching the desired optimal damper displacement vector e_{Tj}, the friction force F_{dj} in the damper is set to its minimum value as in the clipped optimal displacement control strategy. When the jth damper moves in the opposite direction to the optimal damper displacement, the friction force F_{dj} in the damper should be set to a smaller value of the two quantities: F_{max} and the actual damper force $K_{dj}(x_{kj} - x_{kj-1} - e_j)$ minus a small quantity F_o. In this way, the damper is always in motion to dissipate vibration energy. This strategy can be stated as

$$F_{dj} = \begin{cases} F_{min} & \text{when } \dot{e}_j(e_{Tj} - e_j) \succ 0 \\ \min\{\text{abs}[K_{dj}(x_{kj} - x_{kj-1} - e_j)] - F_o,\ F_{max}\} & \text{when } \dot{e}_j(e_{Tj} - e_j) \prec 0 \end{cases} \quad (j = 1, 2, \ldots, m) \tag{24}$$

4. EVALUATION AND COMPARISON

To evaluate the performance of smart dampers in reducing seismic response of frame structures and to compare the efficacy of the three optimal control strategies, an in-depth parameter study is performed on a three-storey shear building with one smart damper installed in the first storey. The building is subjected to an N-S 1940 EI Centro ground excitation. The mass for each floor of the building is taken as 50 t. The horizontal storey stiffness K_1 is 20 800 kN/m. The ratio of the brace horizontal stiffness to the structure horizontal stiffness K_d/K_1 is selected as one. The structural damping is assumed to be Rayleigh damping. The properties of the damper are listed in Table I. The duration and the maximum peak acceleration of the ground motion are taken as 6 and $0.2g$, respectively. The weighting matrix for structural response is selected as

$$[Q] = [\bar{Q}] = \begin{bmatrix} 10000 & 0 & 0 & 0 & 0 & 0 \\ 0 & 1200 & 0 & 0 & 0 & 0 \\ 0 & 0 & 1200 & 0 & 0 & 0 \\ 0 & 0 & 0 & 10000 & 0 & 0 \\ 0 & 0 & 0 & 0 & 1200 & 0 \\ 0 & 0 & 0 & 0 & 0 & 1200 \end{bmatrix} \tag{25}$$

Table I. Basic parameters of smart damper and material used in a three-storey building.

Parameters of smart damper					Parameters of smart material		
L (m)	h (m)	b (m)	A_p (m^2)	P_y (kN)	η (kPa s)	$\tau_{y\min}$ (kPa)	$\tau_{y\max}$ (kPa)
0.5	0.001	0.5	0.01	0.05	0.00017	0.05	10.00

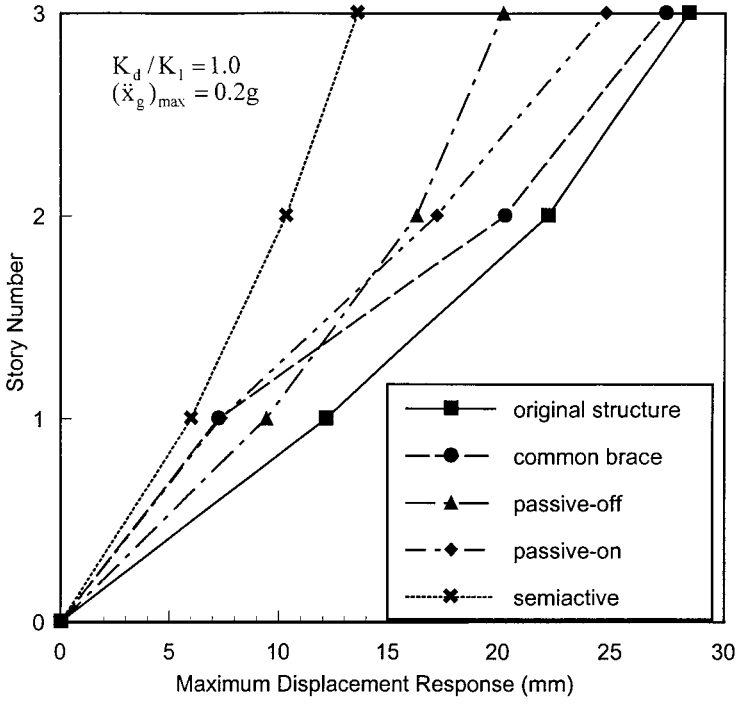

Figure 2. Comparison of maximum displacement response between smart structure and passive structure.

After a parameter study on the weighting coefficients R and $\bar{R}$ in terms of the top floor displacement response of the structure, it is decided to use the same value of 0.0001 for both R and $\bar{R}$ to have a reasonable comparison among the three control strategies.

4.1. Effectiveness of semi-active control

To evaluate the effectiveness of the smart damper for reducing seismic response of the structure, five cases are considered. The first one is the frame structure itself (original structure); the second one is the frame structure with a common brace of stiffness K_d equal to K_1 at the first storey. The third one is the passive-off case in which the applied electric or magnetic field remains constant at the minimum yielding shear stress level. The forth one is the passive-on case in which the applied electric or magnet field remains constant at the maximum yielding shear stress level. The last one is the semi-active control case with the control strategy No. 3. Figure 2 shows the comparison of

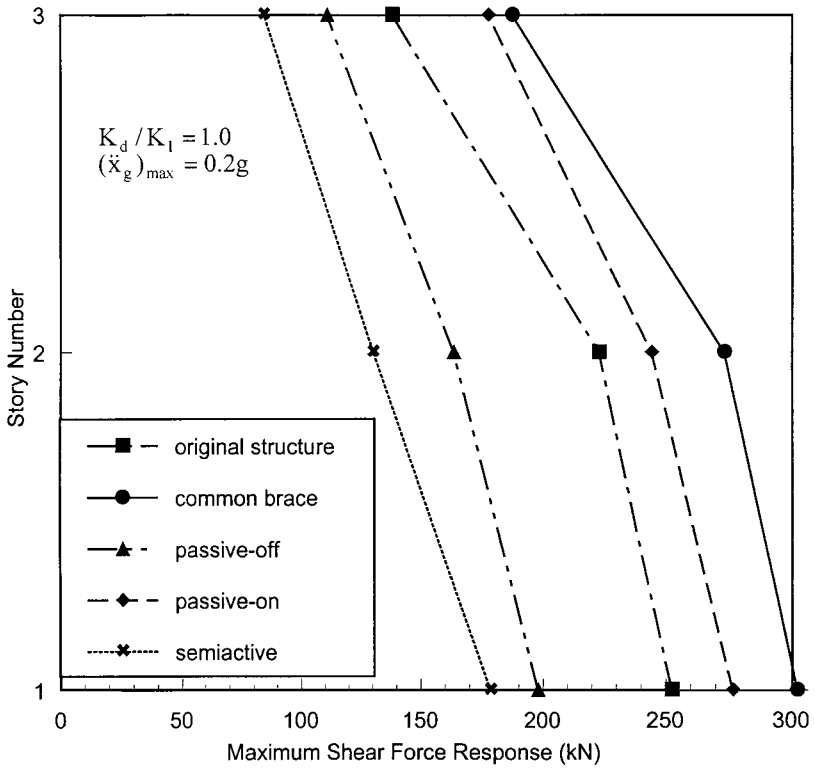

Figure 3. Comparison of maximum shear force response between smart structure and passive structure.

the maximum displacement response at each floor while Figure 3 displays the comparison of the maximum total shear force response (including brace) at each storey. It is seen that though the installation of the common brace or the passive-on damper can reduce the maximum displacement response of each floor, the maximum total shear force at each storey is increased compared with the original structure. The performance of the passive-off damper is better than either the common brace or the passive-on damper because the passive-off damper can dissipate vibration energy as a viscous damper. The smart damper with control strategy No. 3 demonstrates the best performance in that it significantly reduces both the maximum displacement response at each floor and the maximum total shear force at each storey.

4.2. Comparison of three control strategies

To assess the efficacy of three control strategies for the smart damper installed in the first storey of the frame structure, both the maximum displacement response at each floor and the maximum total shear force response at each storey of the system are computed and shown in Figures 4 and 5, respectively, for the selected damper parameters and ground excitation. It is seen that the smart damper with the control strategy No. 2, i.e. the clipped optimal displacement control, can reduce the maximum displacement response at each floor compared with the original structure but not

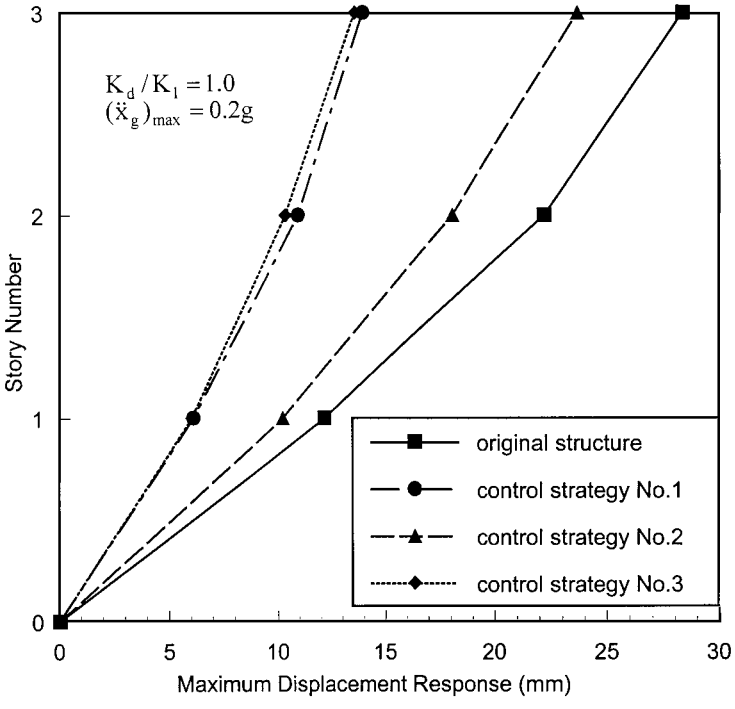

Figure 4. Comparison of control strategies in terms of maximum displacement response.

the maximum shear force at each storey. The smart damper with the control strategy No. 1, that is, the clipped optimal force control, is much better than the smart damper with the control strategy No. 2 in that both the displacement response and the shear force response are significantly reduced. The efficacy of the smart damper with the control strategy No. 3 is slightly superior to the smart damper with the control strategy No. 1. Thus, it can be concluded that the effectiveness of the smart damper in reducing seismic response depends on the used control strategy.

The aforementioned observation on the efficacy of the three control strategies is based on the selected damper parameters. It may change if the damper parameters are altered. The major parameters of a smart damper are the Newtonian viscosity η and the maximum yielding shear stress $\tau_{y\max}$. Thus, it is interesting to know the variations of efficacy of the three control strategies with the maximum yielding shear stress and the Newtonian viscosity of smart fluids. Figure 6 shows the variations of the maximum base shear force (including brace force) with the maximum yielding shear stress for the three control strategies while Figure 7 shows the variations of the maximum damper force with the maximum yielding shear stress. Displayed in Figure 8 are the variations of the maximum base shear force with the Newtonian viscosity. The following phenomena can be observed from these figures.

No matter which control strategy is used, there is an optimal value of $\tau_{y\max}$ by which the best performance of the smart damper can be achieved. The maximum total base shear force can be reduced by 50 per cent if the optimal value of $\tau_{y\max}$ is used. If the maximum yielding shear stress of

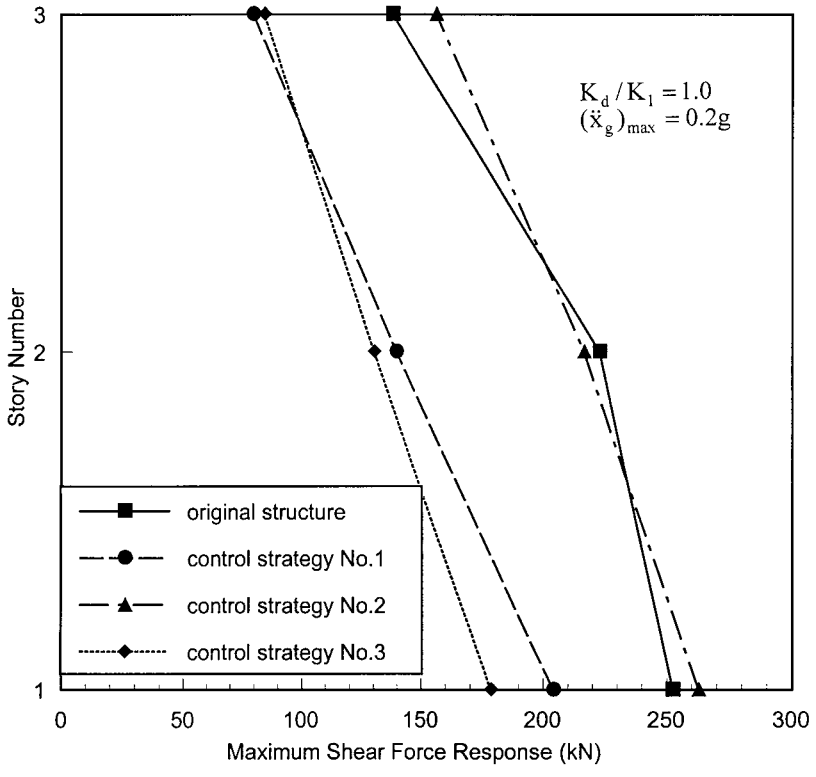

Figure 5. Comparison of control strategies in terms of maximum shear force response.

smart materials is increased after reaching the optimal value, the damper performance will deteriorate until a certain value. After this value, the performance of the damper tends to remain the same. A possible explanation of such a phenomenon for the smart damper with the control strategy Nos. 1 and 2 is that at the optimal value of the smart damper, the probability of the damper force exceeding F_{max} is the highest for the given earthquake intensity and the damper can best dissipate the structural vibration energy. For either the maximum yielding shear stress decreases or increases from the optimal value, the energy dissipation capacity of the damper will deteriorate due to either too small damper force or low probability of the damper force exceeding F_{max}. As the maximum yielding shear stress reaches a certain large value, the probability of the damper force exceeding F_{max} is very small for the given earthquake intensity and the performance of the damper becomes poor. Thus, if the maximum yield shear stress continues to be increases, the smaller probability of the damper force exceeding F_{max} will no longer affect the damper performance. For the smart damper with the control strategy No. 3, the damper can be kept in motion for most of the time. However, after the maximum yielding shear stress reaches a certain level, the damper force will never be larger than F_{max} under the given earthquake intensity. Then, the further increase of the maximum yielding shear stress will not affect the performance of the smart damper with the control strategy No. 3. These observations are consistent with those on the

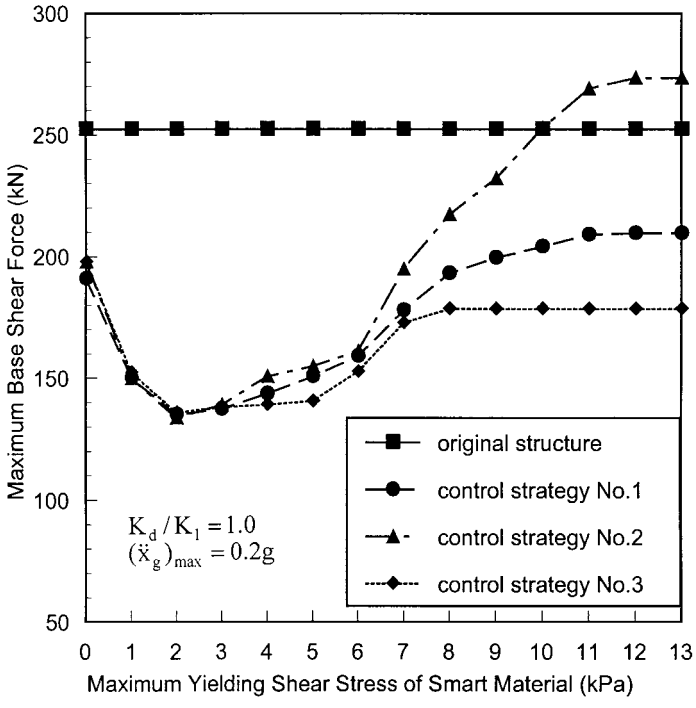

Figure 6. Variations of maximum base shear force with maximum yielding shear stress of smart material.

maximum damper force shown in Figure 7. It can be thus concluded that arbitrarily increasing the maximum yielding shear stress may not be always beneficial, one should select a proper value according to the given structure and given earthquake intensity.

The variations of the maximum base shear force with viscous coefficient of smart material can be observed from Figure 8. For each control strategy, there is an optimal viscous coefficient by which the maximum base shear force reaches its minimum value. This may be because the total damper force consists of the viscous damping force and the friction damping force. The viscous damping force is not adjustable but the friction damping force is controllable. Thus, as the viscous damping force is increased from its optimal value, the function of the controllable friction force will be reduced. On the other hand, the existence of the Newtonian viscosity makes the smart damper to have a stable motion. If it is too small, the effectiveness of the damper will decrease. As a result, there is an optimal value for the Newtonian viscosity in ER fluids or MR fluids.

It is interesting to see from Figures 6 and 7 that when the maximum yielding shear stress is less than 2 or 3 kPa, the performance of the damper is almost the same no matter which control strategy is used. However, with the increase of the maximum yielding shear stress, the performance of the damper with the control strategy No. 3 is the best in terms of the maximum reduction of the maximum base shear force and the minimum damper force generated. It is also seen from Figure 8 that the smart damper with the control strategy No. 3 can have the best

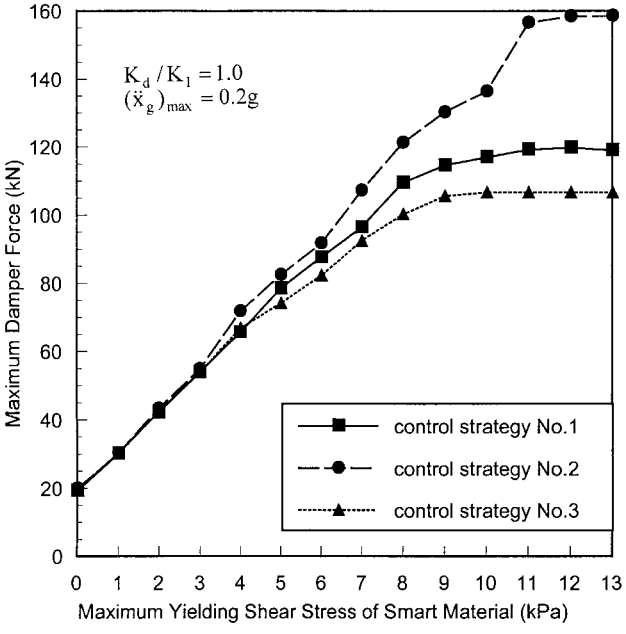

Figure 7. Variations of maximum damper force with maximum yielding shear stress of smart material.

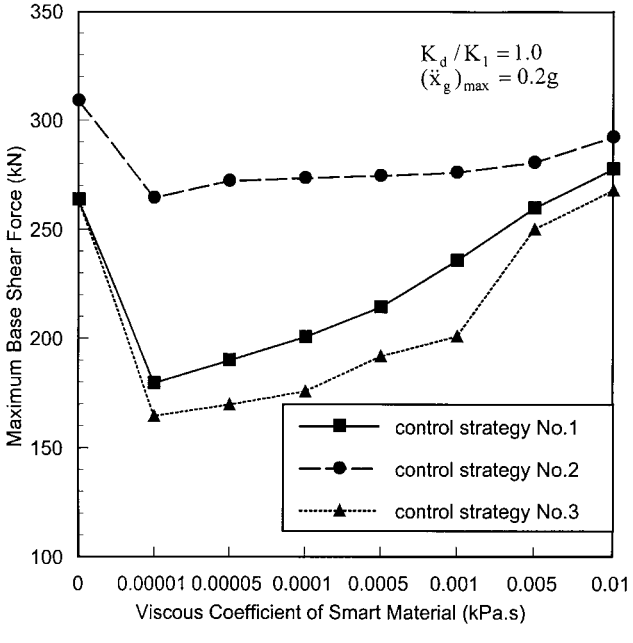

Figure 8. Variations of maximum base shear force with viscous coefficient of smart material.

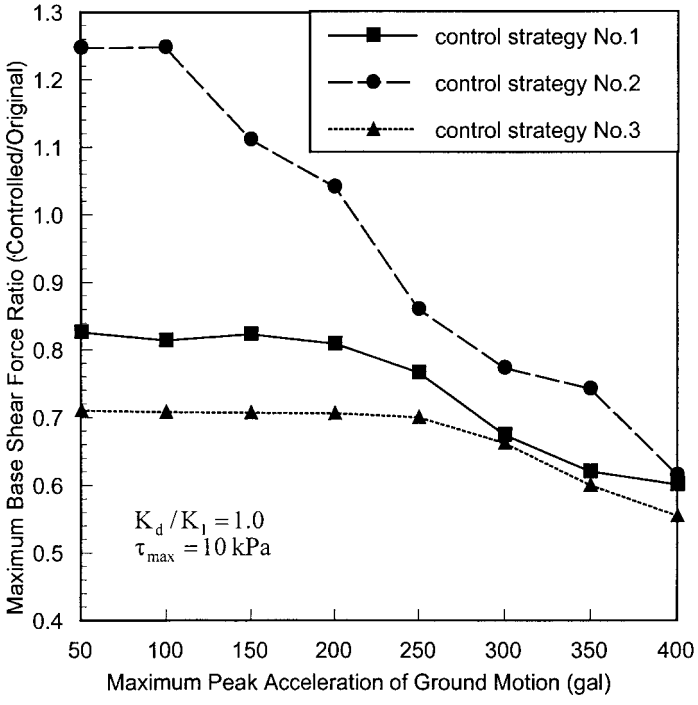

Figure 9. Variations of maximum base shear force ratio with maximum peak acceleration of ground motion

performance related to the Newtonian viscosity. The results presented in Figures 6–8 also indicate that the smart damper with the control strategy No. 3 is least sensitive to the change of the maximum yielding shear stress and the Newtonian viscosity. This character is very useful for the practical implementation of smart dampers.

4.3. Effects of ground excitation and brace stiffness

In the aforementioned discussion, the maximum peak acceleration of the ground motion is taken as $0.2g$. Figure 9 displays the variations of the maximum base shear force ratio of the structure with the maximum peak acceleration of ground motion for $\tau_{y\max}$ equal to 10 kPa. The maximum base shear force ratio here is defined as the ratio of the maximum base shear force of the controlled structure to that of the uncontrolled structure. It is seen that for the small ground acceleration, the smart damper with the control strategy No. 2 behaves like a common brace because of the very low probability of the damper force exceeding $F_{\max}$, and therefore the maximum total base shear force becomes larger than that of the original structure. The smart damper with the control strategy Nos. 1 and 3, however, still works, under the small ground acceleration. When the ground acceleration is increased, the performance of the smart damper is getting better. The performance of the smart damper with the control strategy No. 3 is the best in that it can most reduce the seismic response of the structure and at the same time it is least

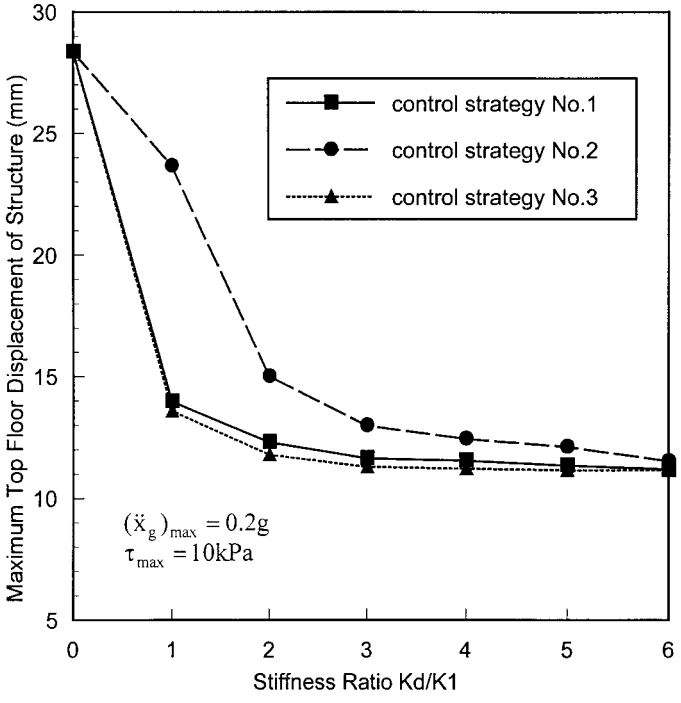

Figure 10. Effects of brace stiffness on control efficiency.

sensitive to the change in the maximum peak acceleration of ground motion. It should be pointed out that $\tau_{y\max}$ used here is fixed but its optimal value actually varies with the maximum peak ground acceleration.

To understand the design criterion of the brace stiffness, the effect of brace stiffness on the reduction of seismic structural response is investigated. Figure 10 shows the variations of the top floor maximum displacement of the structure with stiffness ratio K_d/K_1. It is seen that the stiffness ratio should be as large as possible to achieve the maximum reduction of seismic response. However, when the stiffness ratio reaches above 3, a further increase of the stiffness ratio will not have any further significant response reduction. The poor performance of the smart damper with small brace stiffness is because the soft brace restricts the high damper force to be developed. As a result, the vibration energy dissipation capacity of the damper becomes very poor.

5. APPLICATION

The aforementioned parametric study highlights the importance of the design of smart dampers for a given structure under a given ground motion in order to achieve the maximum structural response reduction. Thus, these findings are applied to a five-storey reinforced concrete building

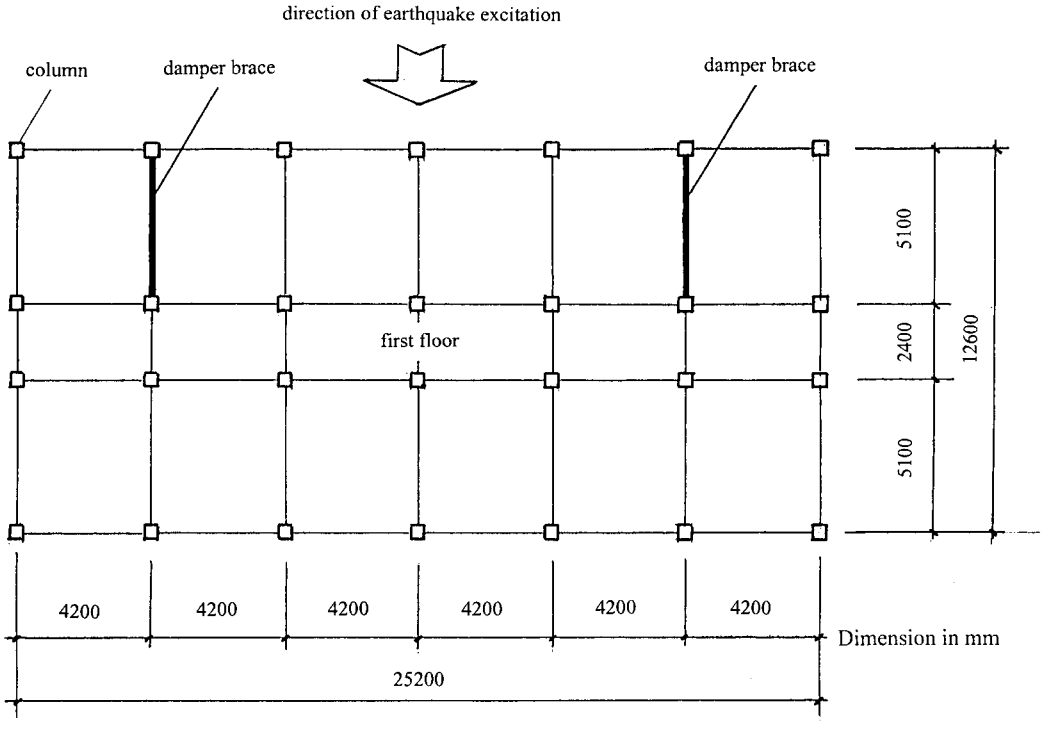

Figure 11. Structural plan of five-storey reinforced concrete building.

Table II. Basic parameters of smart damper and material used in a five-storey building.

Parameters of smart damper					Parameters of smart material		
L (m)	h (m)	b (m)	A_p (m^2)	P_y (kN)	η (kPa s)	$\tau_{y\min}$ (kPa)	$\tau_{y\max}$ (kPa)
0.3	0.001	0.63	0.029	0.3	0.0017	0.05	3.4

subject to an earthquake of fortification intensity 8 as specified in the Chinese code for seismic design of buildings (GBJ 11-89) [17]. The plan dimension of the building structure is shown in Figure 11, and the storey height of the building is 4.2 m. The cross-section of each column is $0.4\,\text{m} \times 0.4\,\text{m}$, and the cross-section of the beam is $025\,\text{m} \times 0.6\,\text{m}$. The Young modulus of the concrete is taken as $2.5 \times 10^7\,\text{kN/m}^2$. The total mass of each floor is about 412.78 t. The two smart ER dampers are installed in the first storey as shown in Figure 11 through the brace system. The dimension of the brace system is shown in Figure 12 and the cross-section of the brace member is $0.15\,\text{m} \times 0.2\,\text{m}$, made of the reinforced concrete. The parametric study of the smart dampers together with some practical restraints result in the design parameters of each damper as listed in Table II.

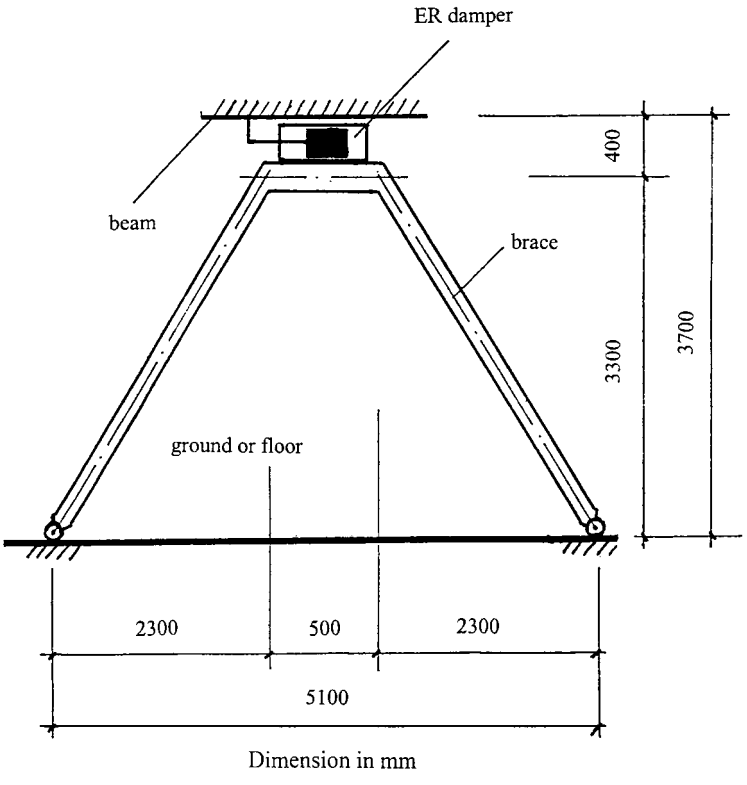

Figure 12. Schematic diagram of ER damper–brace system.

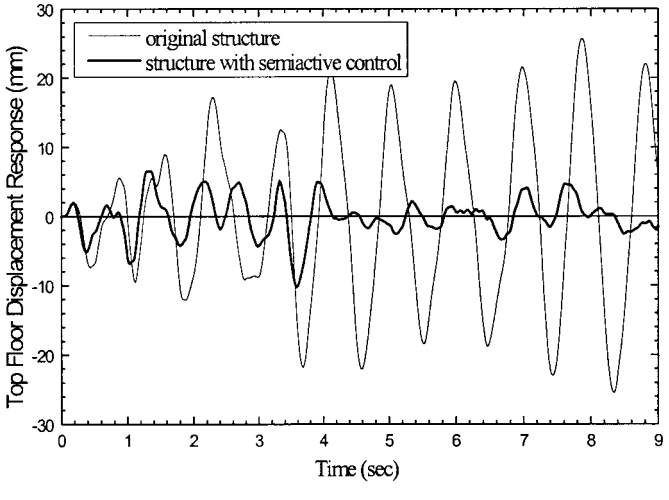

Figure 13. Time-histories of top floor displacement responses.

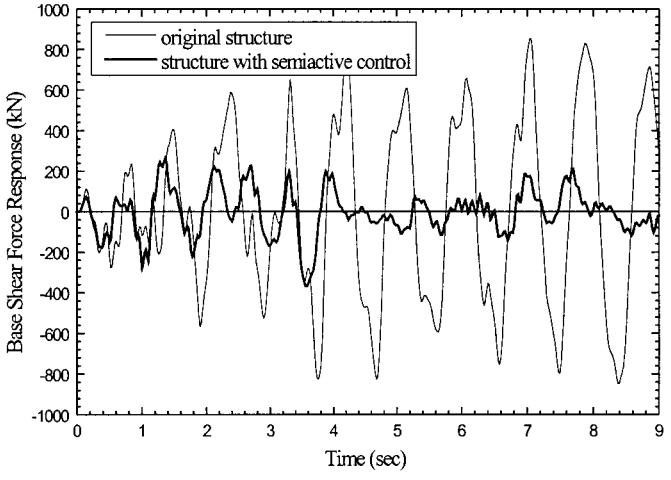

Figure 14. Time-histories of base shear force responses.

The N-S 1940 EI-Centro earthquake excitation is then scaled to one with an equivalent earthquake intensity 8 and is taken as the horizontal ground motion of the building in one direction normal to its wide face, as shown in Figure 11. Only the control strategy No. 3 is used in computation. The time histories of the top floor displacement and base shear force responses of the building with and without semi-active control are shown in Figures 13 and 14, respectively. It is clearly seen that the seismic responses of the building are well controlled by the smart ER dampers, in particular when the building experiences the maximum peak ground acceleration. The maximum base shear force response and the maximum top floor displacement response are reduced by more than 50 per cent. This indicates that for the concerned building, with the two smart ER dampers installed, the intensity of ground acceleration can be reduced by one degree when we carry out the seismic design of the building.

6. CONCLUSIONS

Two optimal displacement control strategies for semi-active control of earthquake-excited structures using ER or MR dampers have been suggested in this study and compared with the optimal force control strategy. The stiffness of the brace system supporting the smart damper has also been taken into consideration. The results show that for a given structure under a given ground motion, no matter which control strategy is used, there exist the optimal values of the maximum yielding shear stress and the Newtonian viscosity of smart fluids, by which the maximum seismic response reduction can be achieved. The smart damper with the optimal displacement control strategy taking the controller–structure interaction into account demonstrated the best performance in terms of structural seismic response reduction and its sensitivity to the environmental change. The performance of smart damper with control strategy was found depending on the earthquake intensity and the stiffness ratio of brace to structure. The work on the example building showed that the installation of smart dampers with proper parameters and

control strategy can significantly reduce the seismic response of the building structure, and the performance of the smart damper is better than that of the common brace or passive device.

ACKNOWLEDGEMENTS

The writers are grateful for the financial support form the Hong Kong Polytechnic University through its Area of Strategic Development Programme in Structural Vibration Control.

REFERENCES

1. Soong TT, Dargush GF. *Passive Energy Dissipation Systems in Structural Engineering*. Wiley & Sons, Chichester, England, 1997.
2. Housner GW, Bergman LA, Caughey TK, Chassiakos AG, Claus RO, Masri SF, Skelton RE, Soong TT, Spencer BF, Yao JTP. Structural control: past present, and future. *Journal of Engineering Mechanics*, ASCE 1997; **123**:897–971.
3. Symans MD, Constantinous MC. Semi-active control systems for seismic protection of structures: a state-of the-art review. *Engineering Structures* 1999; **21**:469–487.
4. Dyke SJ, Spencer BF. Seismic response control using multiple MR dampers. *Proceedings of the 2nd International Workshop on Structural Control*, Hong Kong, 1996a; 163–173.
5. Dyke SJ, Spencer BF, Sain MK, Carlson JD. Modelling and control of magnetorheological dampers for seismic response reduction. *Smart Materials and Structures*, 1996b; **5**:567–575.
6. Carlson JD, Spencer BF. Magnetorheological fluid dampers: scalability and design issues for application to dynamic hazard mitigation. *Proceedings of the 2nd International Workshop on Structural Control*, Hong Kong 1996; 99–109.
7. Spencer BF, Dyke SJ, Sain MK, Carlson JD. Phenomenological model for magnetorheological dampers. *Journal of Engineering Mechanics* 1997; **123**(3):230–238.
8. Spencer BF, Yang GQ, Carlson JD, Sain MK. Smart dampers for seismic protection of structures: a full-scale study. *Proceedings of the 2nd World Conference On Structural Control*, Kyoto, Japan, 1998; 417–426.
9. Ehrgott RC, Masri SF. Modelling the oscillatory dynamic behaviour of electrorheological materials in shear. *Smart Materials and Structures* 1992; **1**(4):275–285.
10. Gavin GP, Hanson RD, Filisko FE. Electrorheological dampers. Part I: analysis and design. *Journal of Applied Mechanics* 1996a; **63**:669–675.
11. Gavin GP, Hanson RD, Filisko FE. Electrorheological dampers. Part I: testing and modelling. *Journal of Applied Mechanics* 1996b; **63**:676–682.
12. Makris N, Burton SA, Hill D, Jordon M. Analysis and design of ER damper for seismic protection of structure. *Journal of Engineering Mechanics* 1996; **122**(10):1003–1011.
13. Ribakov Y, Gluck J. Active control of MDOF structures with supplemental electrorheological fluid dampers. *Earthquake Engineering and Structural Dynamics* 1999; **28**:143–156.
14. Yang JN, Akbarpour A, Ghaemmaghami P. New optimal control algorithms for structural control. *Journal of Engineering Mechanics* 1987; **113**(9):1369–1386.
15. Soong TT. *Active Structural Control*: *Theory and Practice*. Wiley: New York, U.S.A., 1990.
16. Sadek F, Mohraz B. Semiactive control algorithms for structures with variable dampers. *Journal of Engineering Mechanics* 1998; **24**(9):981–990.
17. National Standard of the People's Republic of China. Code for Seismic design of buildings, GBJ 11-89, Ministry of Construction of the Peopel's Republic of China, New World Press, Beijing, China.

